Paramagnetic-to-Antiferromagnetic Phase Boundaries of FeF_2 from Ultrasonic Measurements

Y. Shapira
Francis Bitter National Magnet Laboratory, Massachusetts Institute of Technology, Cambridge, Massachusetts* 02139
(Received 13 May 1970)

The attenuation of longitudinal ultrasonic waves in FeF_2 exhibits a λ anomaly at the paramagnetic-to-antiferromagnetic (P-AF) transition, both in zero and in finite magnetic fields. The P-AF phase boundaries in the H-T plane were determined in magnetic fields up to 200 kG directed along the [001] and [110] directions. These boundaries are well described by the relation $T_N - T = CH^2$, where $C = 10.0 \times 10^{-11}$ °K/G^2 for $\vec{H} \parallel [001]$, and $C = 2.0 \times 10^{-11}$ °K/G^2 for $\vec{H} \parallel [110]$. The Néel temperature is $T_N = (78.35 \pm 0.03)$ °K. The experimental results for the P-AF phase boundaries are in reasonable agreement with the results of detailed calculations carried out in the molecular field approximation. These calculations include the effects of the anisotropy on T_N, and on the coefficient C for fields parallel and perpendicular to the preferred axis. The more general problem of the effect of a single-ion anisotropy on the response of a spin to an effective magnetic field is also considered. A thermodynamic relation, derived by Skalyo *et al.*, for the P-AF phase boundary with $\vec{H} \parallel [001]$ is fairly well satisfied. An unusual behavior was observed for longitudinal waves propagating along [110] with $\vec{H}$ along [001]. In this configuration, the magnitude of the λ anomaly in the attenuation, at the P-AF phase boundary, increased rapidly with H.

I. INTRODUCTION

Magnetic phase transitions in the ideal uniaxial antiferromagnet MnF_2 were recently studied using ultrasonic and differential magnetization techniques. The theory of the various phase transitions which occur in a simple uniaxial antiferromagnet was reviewed in that paper. The present paper on FeF_2 is a natural extension of the work on MnF_2 to a similar, but somewhat more complicated, antiferromagnet. Much of the background material for the present work is covered in Ref. 1 and will not be repeated here. A preliminary report on the experimental results in FeF_2 was published earlier.[2]

FeF_2 has a rutile structure with the Fe^{++} ions on a body-centered tetragonal lattice. At low temperatures, FeF_2 is a simple two-sublattice antiferromagnet in which the preferred direction for the spins is the [001] direction (tetragonal axis, or c axis). The anisotropy in FeF_2 arises mainly from the interaction of each Fe^{++} ion with its crystalline environment. This interaction is well represented by a term of the form $-DS_z^2$ in the Hamiltonian, where $D = 6.5$ cm^{-1} and S_z is the component of the spin along the tetragonal axis.[3-5] For Fe^{++}, the spin quantum number is $S = 2$. The exchange interaction in FeF_2 is due primarily to the interaction of each cation with eight next-nearest neighbors on the opposite sublattice.[4,5] If the cation in question is at (0, 0, 0), then the next-nearest neighbors are at $(\pm\frac{1}{2}, \pm\frac{1}{2}, \pm\frac{1}{2})$. The intrasublattice exchange interaction is much smaller than the intersublattice exchange interaction. The Néel temperature is $T_N = 78.35$ °K.[6]

There is a great deal of similarity between FeF_2 and MnF_2. Both have rutile structure, both are uniaxial antiferromagnets with the [001] axis as the preferred direction for the spins, and they have comparable exchange interactions and Néel temperatures ($T_N = 67.3$ °K for MnF_2). The main difference between the magnetic interactions in the two materials is the difference in the anisotropy. In MnF_2 the anisotropy is small and it arises mainly from magnetic dipole-dipole interaction,[7] whereas in FeF_2 the anisotropy is much larger and it arises mainly from the interaction of a single ion with its crystalline environment.

The present paper is devoted primarily to the experimental determination of the paramagnetic-to-antiferromagnetic phase boundaries (in the H-T plane) in FeF_2. These boundaries were determined from experiments with longitudinal ultrasonic waves in which the paramagnetic-to-antiferromagnetic (hereafter P-AF) transition appeared as a λ-type peak in the ultrasonic attenuation. An unusual behavior of the magnitude of this λ-type peak is also reported. In addition, a detailed calculation of the effects of a single-ion anisotropy on the P-AF phase boundaries is carried out in the Appendix using the molecular field approximation. The calculation starts by considering the effect of a single-ion anisotropy on the response of a spin to an effective magnetic field. The treatment is then specialized to the effect of the anisotropy on T_N and on the curvature of the P-AF phase boundaries for fields parallel and perpendicular to the preferred axis. The effects of the anisotropy are taken into account only to first order in D/kT_N.

The paper is arranged as follows. The theory for the P-AF phase boundaries is discussed briefly in Sec. II, and also in the Appendix. Section III is devoted to experimental techniques. The experimental results are presented in Sec. IV and are discussed in Sec. V.

II. THEORY

The theory of phase transitions of a uniaxial antiferromagnet of the easy-axis type is reviewed in Ref. 1. Of the various phase transitions which are possible, the only ones which are of immediate concern are the transitions from the paramagnetic (P) phase to the antiferromagnetic (AF) phase for fields parallel and perpendicular to the preferred axis. Other transitions should occur at fields above those which were available in the present study. Some theoretical results for the P-AF transitions are reproduced below. In this discussion, a direction along the preferred axis will be represented by the unit vector $\vec{n}$.

Calculations based on several models indicate that the temperature T at the P-AF transition decreases monotonically as the magnetic field H increases. Exact theoretical solutions for the P-AF phase boundary, in the H-T plane, are not available at present. There are, however, some results which are based on certain models and simplifying assumptions. In particular, the P-AF boundary was calculated in the molecular field approximation (hereafter MFA) for the case when the anisotropy interaction is small compared to the exchange interaction. The result for the P-AF boundary at temperatures just below T_N is

$$T_N - T = CH^2, \tag{1}$$

where the coefficient C depends on the exchange constants and on the angle between $\vec{H}$ and $\vec{n}$. In FeF_2, the intrasublattice exchange interaction is very small compared to the intersublattice exchange interaction.[4,5] In this case the coefficient C for $\vec{H} \parallel \vec{n}$ is given by

$$C_{\parallel} = \frac{3g_{\parallel}^2 \mu_B^2 (2S^2 + 2S + 1)}{80 k z_1 |J_1| S(S+1)}, \tag{2}$$

where S is the spin quantum number ($S = 2$ for Fe^{++}), μ_B is the Bohr magneton, $g_{\parallel}$ is the g factor for $\vec{H} \parallel \vec{n}$, k is the Boltzmann constant, z_1 is the number of neighbors on the opposite sublattice which interact with a given magnetic ion, and J_1 is the exchange constant. It should be noted that the exchange interaction between two interacting ions on opposite sublattices is taken to be $-2J_1 \vec{S}_1 \cdot \vec{S}_2$, whereas some authors take it to be $J_1 \vec{S}_1 \cdot \vec{S}_2$. In the case $\vec{H} \perp \vec{n}$ the coefficient C is given by

$$C_{\perp} = \frac{g_{\perp}^2 \mu_B^2 (2S^2 + 2S + 1)}{80 k z_1 |J_1| S(S+1)}, \tag{3}$$

where $g_{\perp}$ is the g factor for $\vec{H} \perp \vec{n}$.

Equations (2) and (3) can be rewritten in a different form by using the relation

$$kT_N = \tfrac{2}{3} S(S+1) z_1 |J_1|, \tag{4}$$

which enables one to express $|J_1|$ in terms of T_N. It should be noted, however, that relation (4) holds only in the MFA and when the anisotropy interaction is negligible compared to the exchange interaction. In practice, if one uses the experimental value of T_N and the value of J_1 obtained from neutron diffraction, then the left and right sides of Eq. (4) may differ appreciably. In that case, the molecular field equations for $C_{\parallel}$ and $C_{\perp}$ when expressed in terms of J_1 will lead to numerical results which differ from those obtained from the expressions for $C_{\parallel}$ and $C_{\perp}$ in terms of T_N. In calculating $C_{\parallel}$ and $C_{\perp}$ for the case of no anisotropy, we shall use expressions (2) and (3) which relate $C_{\parallel}$ and $C_{\perp}$ to J_1.

In FeF_2, the anisotropy interaction is not negligible compared to the exchange interaction, and it should therefore be included in the calculation of $C_{\parallel}$ and $C_{\perp}$. In the Appendix, we consider the effect of a single-ion anisotropy interaction, of the form DS_z^2, on $C_{\parallel}$ and $C_{\perp}$. The calculations are carried out in the MFA and only to first order in DS^2/kT_N. Thus, aside from the inherent limitations of the MFA, the calculations in the Appendix are limited to the case $DS^2/kT_N \ll 1$. In FeF_2, however, $DS^2/kT_N \approx 0.5$. If one applied the results in the Appendix to FeF_2 one concludes that the anisotropy changes $C_{\parallel}$ by less than ~5%, but decreases $C_{\perp}$ by ~11%. Using a computer, Misetich[8] has calculated the P-AF boundary in FeF_2 in the MFA. These calculations were performed only for the case $\vec{H} \parallel \vec{n}$ and included the anisotropy interaction to all orders. The results indicate that the anisotropy changes $C_{\parallel}$ by less than 2%.

The discussion thus far was based on the MFA. A more general thermodynamic relation was derived by Skaylo *et al.*[9] for the case $\vec{H} \parallel \vec{n}$. This relation uses a result by Fisher,[10] according to which the magnetic contribution to the specific heat C_m (at $H = 0$) is related to the susceptibility $\chi_{\parallel}$ (for $\vec{H} \parallel \vec{n}$) by the equation

$$C_m = A \frac{\partial [T\chi_{\parallel}(T)]}{\partial T}, \tag{5}$$

where A is a slowly varying function of T near T_N. Assuming that Eq. (5) is valid near T_N, Skaylo *et al.* showed that for T just below T_N, the P-AF boundary for the case $\vec{H} \parallel \vec{n}$ obeys the relation

$$\frac{d^2T}{dH^2} = -A^{-1}. \tag{6}$$

III. EXPERIMENTAL PROCEDURE

Ultrasonic-attenuation measurements were per-

formed on a single crystal of FeF_2 grown by Guggenheim at the Bell Telephone Laboratories and obtained from Chinn of Lincoln Laboratory. The sample was approximately cubic with an edge of ~1 cm. The faces of the sample, which were normal to the [110], [1$\bar{1}$0], and [001] directions, were polished for ultrasonic work.

The attenuation of 10- to 50-MHz longitudinal waves propagating along the [110] and [001] directions was measured using pulse techniques. The sound waves were generated with X-cut quartz transducers which were bonded to the sample with Dow Corning 200 silicone fluid having a viscosity of 30 000 cS at 25 °C. The attenuation was usually measured as a function of T at constant H, although some measurements of the attenuation as a function of H at constant T were also made.

All experiments were performed with the sample immersed in liquid nitrogen. The temperature was varied either by pumping on the nitrogen bath or by raising the vapor pressure over the nitrogen bath above 760 Torr using compressed nitrogen gas. Temperatures were measured with a platinum resistance thermometer, as described in Ref. 1, to an accuracy of 0.03 °K at $H = 0$, and 0.05 °K at high fields.

Steady magnetic fields up to 200 kG were produced by Bitter-type solenoids. The applied magnetic field was known to an accuracy of ~0.5%. The demagnetizing field in the sample was estimated to be sufficiently small so that the internal field inside the sample differed from the applied magnetic field by less than ~1%. In analyzing the data the demagnetizing field was ignored and no distinction was made between the internal and applied fields.

IV. EXPERIMENTAL RESULTS

Experiments were carried out with ultrasonic waves propagating along the [001] and [110] directions. The various modes of sound propagation along these directions, and their velocities at 77.6 °K, are listed in Table I. Each mode is characterized by the direction of its propagation vector $\vec{q}$ and by the direction of ion displacement $\vec{\xi}$. The velocities, which were measured to an accuracy of 2%, are fairly close to those observed in MnF_2.[11]

TABLE I. The velocity of sound V at 77.6 °K for several modes of propagation.

$\vec{q}$	$\vec{\xi}$	Type of mode	$V(10^5$ cm/sec)
[001]	[001]	longitudinal	6.4
[001]	in (001) plane	shear	2.92
[110]	[110]	longitudinal	6.6
[110]	[001]	shear	2.92
[110]	[1$\bar{1}$0]	shear	1.77

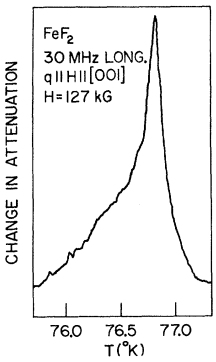

FIG. 1. Recorder tracing of the attenuation of 30-MHz longitudinal ultrasonic waves near the P-AF phase boundary with $\vec{H} \parallel [001]$. The trace was obtained by keeping H at 127 kG and varying T.

The P-AF boundaries in the H-T plane were determined from attenuation measurements with longitudinal ultrasonic waves, carried out with $\vec{H}$ along either the [001] or the [110] directions. The results for the P-AF boundaries for the two field directions are described separately. An unusual behavior observed for one mode of propagation is described later.

A. P-AF Boundary with $\vec{H}$ along [001]

Measurements of the attenuation as a function of T at constant H, and as a function of H at constant T, were carried out with 10-, 30-, and 50-MHz longitudinal waves propagating along the [001] and [110] directions. A λ-type peak in the attenuation was observed at the P-AF transition. Figure 1 shows a recorder tracing of this peak. Within experimental accuracy, the position of the attenuation peak in the H-T plane was independent of frequency and direction of propagation of the ultrasonic wave. The results at $H = 0$ gave the value $T_N = (78.35 \pm 0.03)$ °K for the Néel temperature. This value agrees with the one obtained from specific-heat measurements.[6]

The results for the P-AF boundary in the H-T plane are shown in Fig. 2. These data were fitted to the equations

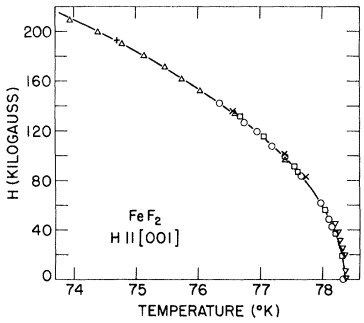

FIG. 2. P-AF phase boundary for $\vec{H} \parallel [001]$. The solid curve is the best fit to Eq. (1) with $C = 9.95 \times 10^{-11}$ °K/G^2.

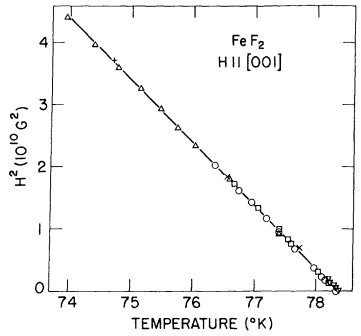

FIG. 3. A plot of H^2 versus T for the P-AF boundary with $\vec{H} \parallel [001]$. The solid line is the best fit to Eq. (1) with $C = 9.95 \times 10^{-11}$ °K/G^2.

$$T_N - T = C_1 H^2 \tag{7}$$

and

$$T_N - T = C_1 H^2 + C_2 H^4, \tag{8}$$

using the least-squares method and treating T_N and C_i as adjustable parameters. For Eq. (7) we obtained $T_N = (78.364 \pm 0.012)$ °K and $C_1 = (9.952 \pm 0.069) \times 10^{-11}$ °K/G^2, with an rms residual of 0.027 °K, and a largest residual of 0.059 °K. For Eq. (8) we obtained $T_N = (78.357 \pm 0.014)$ °K, $C_1 = (9.771 \pm 0.21) \times 10^{-11}$ °K/G^2, and $C_2 = (4.9 \pm 5.5) \times 10^{-23}$ °K/G^4, with an rms residual of 0.026 °K, and a largest residual of 0.056 °K. Note that, even at 200 kG, the magnitude of the term $C_2 H^4$ in Eq. (8) is only 2% of the value for $C_1 H^2$, so that $T_N - T$ is closely proportional to H^2 for fields up to 200 kG. A plot of H^2 versus T is shown in Fig. 3.

B. P-AF Boundary with $\vec{H}$ along [110]

Measurements with 10–50-MHz longitudinal

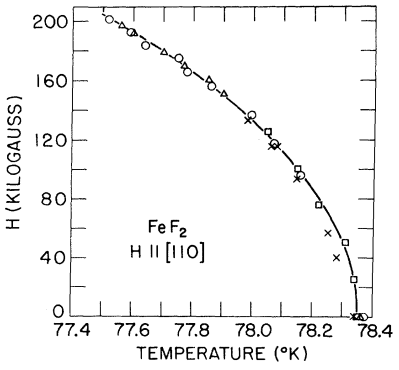

FIG. 4. P-AF phase boundary for $\vec{H} \parallel [110]$. The solid curve is the best fit to Eq. (1) with $C = 2.014 \times 10^{-11}$ °K/G^2.

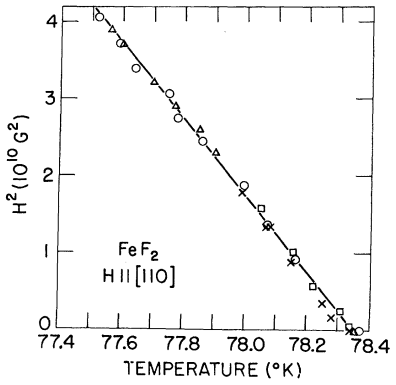

FIG. 5. A plot of H^2 versus T for the P-AF boundary with $\vec{H} \parallel [110]$. The solid line is the best fit to Eq. (1) with $C = 2.014 \times 10^{-11}$ °K/G^2.

waves propagating along the [110] and [001] directions indicate that the P-AF transition is accompanied by a λ-type peak in the ultrasonic attenuation. The results for the P-AF boundary obtained from these measurements are shown in Fig. 4.

The data for the P-AF boundary were fitted to Eqs. (7) and (8). The best fit to Eq. (7) gave $T_N = (78.346 \pm 0.002)$ °K and $C_1 = (2.014 \pm 0.008) \times 10^{-11}$ °K/G^2, with an rms residual of 0.015 °K, and a largest residual of 0.033 °K. The best fit to Eq. (8) gave $T_N = (78.344 \pm 0.002)$ °K, $C_1 = (1.959 \pm 0.028) \times 10^{-11}$ °K/G^2, and $C_2 = (1.47 \pm 0.72) \times 10^{-23}$ °K/G^4, with an rms residual of 0.014 °K, and a largest residual of 0.031 °K. At 200 kG, the magnitude of the term $C_2 H^4$ in Eq. (8) is only 3% of the value for the $C_1 H^2$ term. A plot of H^2 versus T is shown in Fig. 5.

C. Magnitude of λ Peaks

For a given magnetic field $\vec{H}$, the attenuation of longitudinal waves as a function of temperature exhibits a λ-type peak at the P-AF transition. The magnitude $\Delta\alpha(H)$ of this peak is taken to be the difference between the attenuation at the P-AF transition temperature (for a given $\vec{H}$) and the attenuation at much higher temperatures.

Some observations of the variation of $\Delta\alpha(H)$ with H were made for the following situations: (1) $\vec{q} \parallel [001]$, $\vec{H} \parallel [001]$; (2) $\vec{q} \parallel [001]$, $\vec{H} \parallel [110]$; (3) $\vec{q} \parallel [110]$, $\vec{H} \parallel [110]$; and (4) $\vec{q} \parallel [110]$, $\vec{H} \parallel [001]$. Here, the longitudinal mode is characterized by its propagation vector $\vec{q}$. For the first three configurations listed above it was found that $\Delta\alpha$ was more or less independent of H. For example, for 30-MHz longitudinal waves with both $\vec{q}$ and $\vec{H}$ along [001], $\Delta\alpha(H)$ was approximately 3 dB/cm for all values of H.

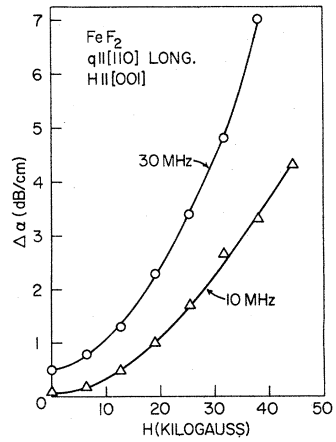

FIG. 6. Magnetic field variation of the magnitude $\Delta\alpha(H)$ of the λ peak for 10- and 30-MHz longitudinal waves with $\vec{q} \parallel [110]$ and $\vec{H} \parallel [001]$.

A striking variation of $\Delta\alpha(H)$ with H was observed in the case $\vec{q} \parallel [110]$ and $\vec{H} \parallel [001]$. In this configuration $\Delta\alpha(H)$ increased rapidly as H was increased. Figure 6 shows the results obtained with 10- and 30-MHz longitudinal waves. For the 10-MHz wave, $\Delta\alpha$ at 44.5 kG is about 60 times greater than at $H = 0$. This rapid increase of $\Delta\alpha$ with H was not observed in similar experiments which we performed in MnF_2.

V. DISCUSSION

In this section, we first discuss briefly the λ anomalies in the ultrasonic attenuation, and then compare the observed P-AF phase boundaries with theory.

A. λ Anomalies in Attenuation

The observation of λ anomalies in the attenuation of longitudinal sound waves near the P-AF phase boundaries is in line with earlier observations in MnF_2.[1] Such λ anomalies are often observed near second-order phase transitions, such as the Curie point in ferromagnets,[12] the λ point in liquid helium,[13] and the P-AF transitions in antiferromagnets. The magnitudes $\Delta\alpha$ of the attenuation peaks near the Néel point of FeF_2 are comparable to, but smaller than, those observed in MnF_2. For a 30-MHz longitudinal wave propagating along [001] at $H = 0$, $\Delta\alpha \approx 3$ dB/cm for FeF_2, as compared to $\Delta\alpha \approx 5$ dB/cm for MnF_2. For a 30-MHz longitudinal wave with $\vec{q} \parallel [110]$, $\Delta\alpha \approx 0.5$ dB/cm for FeF_2 (at $H = 0$), while $\Delta\alpha \approx 1.5$ dB/cm for MnF_2. In comparing the magnitudes of $\Delta\alpha$ for FeF_2 and MnF_2, one should keep in mind the possibility that $\Delta\alpha$ depends on the particular single crystal which is used in the experiment.

Perhaps the most interesting aspect of the λ anomalies observed in this study is the H dependence of $\Delta\alpha(H)$ for the longitudinal mode with $\vec{q} \parallel [110]$ when $\vec{H}$ is along [001]. The rapid increase of $\Delta\alpha$ with H in this case occurs only in FeF_2, but not in MnF_2. The origin of this phenomenon is not known at present.

B. P-AF Phase Boundaries

The P-AF phase boundaries in FeF_2, for fields up to 200 kG directed along the [001] and [110] directions, are reasonably well described by molecular field theory. Qualitatively, for both phase boundaries, $T_N - T$ is proportional to H^2 (see Figs. 3 and 5) in accordance with Eq. (1). To make a quantitative comparison between molecular field theory and experiment, we first evaluated the right-hand sides of Eqs. (2) and (3) and then used the results in the Appendix to correct for the effects of the anisotropy. Using $S = 2$, Lines's values[4] $g_\parallel = 2.21$, $g_\perp = 2.08$, and the neutron diffraction value[5] $J_1 = -1.82\ \mathrm{cm}^{-1}$, we obtained from Eqs. (2) and (3) $C_\parallel = 8.55 \times 10^{-11}\ ^\circ\mathrm{K/G}^2$ and $C_\perp = 2.52 \times 10^{-11}\ ^\circ\mathrm{K/G}^2$. The calculations in the Appendix, which are based on the MFA, indicate that the anisotropy changes $C_\parallel$ by less than ~5% and decreases $C_\perp$ by ~11%. The computer calculations by Misetich[8] indicate that the anisotropy changes $C_\parallel$ by less than 2%. Hence, molecular field theory gives $C_\parallel \approx 8.6 \times 10^{-11}\ ^\circ\mathrm{K/G}^2$, and $C_\perp \approx 2.2 \times 10^{-11}\ ^\circ\mathrm{K/G}^2$. These values should be compared to the value $C_\parallel = 9.95 \times 10^{-11}\ ^\circ\mathrm{K/G}^2$ and $C_\perp = 2.01 \times 10^{-11}\ ^\circ\mathrm{K/G}^2$ obtained from best fits of the data to Eq. (7). Fits of the data to Eq. (8) gave $C_\parallel = 9.77 \times 10^{-11}\ ^\circ\mathrm{K/G}^2$ and $C_\perp = 1.96 \times 10^{-11}\ ^\circ\mathrm{K/G}^2$, where $C_\parallel$ was identified with $\lim (T_N - T)/H^2$ as $H \to 0$ for $\vec{H} \parallel [001]$, and similarly for $C_\perp$. The above values show that the predictions of the molecular field theory for the coefficients $C_\parallel$ and $C_\perp$ are within ~15% of the experimental values. This agreement is surprisingly good in view of the fact that in MnF_2 the differences between molecular field theory and experiment are much larger.[1] For the Néel temperature of FeF_2, the molecular field theory (including the corrections for the anisotropy) gives a value which is about 20% higher than the experimental value.

Theoretically, the curvature of the P-AF boundary at T_N, when $\vec{H}$ is along [001], is related to the specific heat and to the susceptibility by Eqs. (5) and (6). To test this prediction we analyzed the specific-heat data of Catalano and Stout[6] together with the susceptibility data of Stout and Yuzuri.[14] These data seem to indicate that relation (5) holds for FeF_2 with $A \cong 4.3 \times 10^9\ \mathrm{G}^2/^\circ\mathrm{K}$ near T_N. The same estimate for A was obtained when the specific-heat data of Catalano and Stout were combined with the susceptibility data of Foner.[15] Using Eq. (6) one then obtains for the curvature at

T_N the value $d^2T/dH^2 \cong -2.3\times10^{-10}\,^\circ\mathrm{K/G^2}$. The best fits of the experimental data to Eqs. (7) and (8) lead to $d^2T/dH^2 = -1.99\times10^{-10}\,^\circ\mathrm{K/G^2}$ and $d^2T/dH^2 = -1.95\times10^{-10}\,^\circ\mathrm{K/G^2}$ at T_N, respectively. It thus appears that the thermodynamic relation given by Eq. (6) is in reasonably good agreement with the present data.

ACKNOWLEDGMENTS

The author is indebted to H. J. Guggenheim and S. R. Chinn for the single crystal of FeF_2, to A. Misetich for computer calculations, to D. R. Nelson for programming, to S. Foner, H. C. Praddaude, and D. J. Kim for many useful discussions, to L. G. Rubin for advice on thermometry, and to V. Diorio for technical assistance.

APPENDIX: EFFECT OF SINGLE-ION ANISOTROPY ON P-AF PHASE BOUNDARIES

The P-AF phase boundaries in a simple two-sublattice uniaxial antiferromagnet were discussed in Ref. 1. An explicit calculation of these phase boundaries was carried out in the Appendix of that reference for the special case of a negligibly small anisotropy and a negligibly small intrasublattice exchange interaction. These calculations were carried out using the MFA and specializing to temperatures near T_N and to the configurations $\vec{H}\parallel\vec{n}$ and $\vec{H}\perp\vec{n}$. Here we generalize the results to include the effects of a single-ion anisotropy, of the form DS_z^2, on the P-AF boundaries near T_N. The calculations will be carried out in the MFA and only to first order in DS^2/kT_N.

A schematic of the magnetic phase diagram of a simple uniaxial antiferromagnet at temperatures near T_N is shown in Fig. 7. For $\vec{H}\parallel\vec{n}$, there are three phases: paramagnetic (P), antiferromagnetic (AF), and spin-flop (SF). For $\vec{H}\perp\vec{n}$, there are only two phases: P and AF (see Ref. 1). The presence of a small single-ion anisotropy of the form DS_z^2 influences the magnetic phase diagram in several ways. First, the Néel temperature changes from the value $T_N(0)$ for the case of no anisotropy to a higher value $T_N(D)$. This was considered by Ohlmann and Tinkham,[3] and by others.[4,16] Second, for either $\vec{H}\parallel\vec{n}$ or $\vec{H}\perp\vec{n}$, the coefficient C which appears in Eq. (1) for the P-AF boundary is changed somewhat by the anisotropy. Third, the boundary between the SF and P phases, for $\vec{H}\parallel\vec{n}$, is slightly affected by the anisotropy. Finally, the boundary between the AF and SF phases, for $\vec{H}\parallel\vec{n}$, depends strongly on the anisotropy, as discussed by Yosida.[17] Here we shall be concerned only with effect of the anisotropy on the P-AF phase boundaries for $\vec{H}\parallel\vec{n}$ and $\vec{H}\perp\vec{n}$. This includes the change in the Néel temperature, and the change in the coefficients $C_\parallel$ and $C_\perp$.

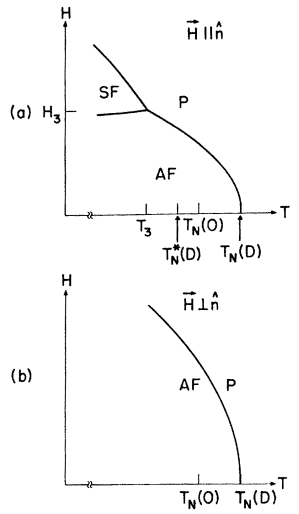

FIG. 7. Schematic phase diagram for a uniaxial antiferromagnet (of the easy-axis type) with weak anistropy: (a) $\vec{H}\parallel\vec{n}$; (b) $\vec{H}\perp\vec{n}$. This schematic shows the phase diagram only at temperatures near $T_N(D)$.

A. Response Functions

Consider a system of independent spins which is acted on by an effective magnetic field $\vec{H}_{eff}$ in the absence of anisotropy. The average magnetic moment $\bar{\mu}$ per spin is directed along $\vec{H}_{eff}$ and is given by

$$\bar{\mu} = \mu_0 B_S(x), \tag{A1}$$

where $\mu_0 = g\mu_B S$, $x = \mu_0 H_{eff}/kT$, and $B_S(x)$ is the Brillouin function for spin S. In calculating the P-AF phase boundaries near T_N one expands $B_S(x)$ in powers of x and retains only the two leading terms. This leads to the expression

$$\bar{\mu} = \mu_0\left(\frac{S+1}{3S}\,x - \frac{(S+1)(2S^2+2S+1)}{90S^3}\,x^3\right). \tag{A2}$$

Equation (A2) describes the response of a spin to an effective magnetic field where there is no anisotropy. For $S=1$, Eq. (A2) gives

$$\bar{\mu} = \mu_0\left[\frac{2\mu_0 H_{eff}}{3kT} - \frac{1}{9}\left(\frac{\mu_0 H_{eff}}{kT}\right)^3\right] \quad (S=1). \tag{A3}$$

For $S=2$, which is applicable to FeF_2, Eq. (A2) gives

$$\bar{\mu} = \mu_0\left[\frac{\mu_0 H_{eff}}{2kT} - \frac{13}{240}\left(\frac{\mu_0 H_{eff}}{kT}\right)^3\right] \quad (S=2). \tag{A4}$$

In the classical limit ($S=\infty$),

$$\bar{\mu} = \mu_0\left[\frac{\mu_0 H_{eff}}{3kT} - \frac{1}{45}\left(\frac{\mu_0 H_{eff}}{kT}\right)^3\right] \quad (S=\infty). \tag{A5}$$

We proceed to calculate the analog of Eq. (A2) in

the presence of anisotropy.

1. $\vec{H}_{eff} \| \vec{n}$

Let the anisotropy energy be $-DS_z^2$, where the z direction is along $\vec{n}$. The Hamiltonian for a spin is

$$\mathcal{H} = -\vec{\mu} \cdot \vec{H}_{eff} - DS_z^2 , \tag{A6}$$

where $\vec{\mu} = g\mu_B \vec{S}$. Let $|m\rangle$ be the eigenstates of the operators S_z and S^2 with eigenvalues m and $S(S+1)$, respectively. When $\vec{H}_{eff}$ is along $\vec{n}$ the average moment per spin is directed along $\vec{n}$ and is given by

$$\bar{\mu} = \frac{\mu_0}{S} \frac{\sum_m m \exp[(mg\mu_B H_{eff} + Dm^2)/kT]}{\sum_m \exp[(mg\mu_B H_{eff} + Dm^2)/kT]} . \tag{A7}$$

In evaluating the ratio of the two sums in Eq. (A7) we shall make expansions which involve the paramters $x = \mu_0 H_{eff}/kT$ and $y = DS^2/kT$. We assume that both of these parameters are small compared to unity and retain terms up to order x^3 and up to order y. Thus the effect of anisotropy is considered only to first order in DS^2/kT.

Before evaluating Eq. (A7) for special cases, it is useful to note that $\bar{\mu}$ is an odd function of H_{eff} because the average moment must reverse its sign when the effective field is reversed. Furthermore, apart from numerical factors, the sums in Eq. (A7) always include H_{eff} only in the ratio $x = \mu_0 H_{eff}/kT$. It follows that if one expands Eq. (A7) in powers of x keeping terms up to x^3, then one obtains the form

$$\bar{\mu} = \mu_0 (A_1 x + A_2 x^3) , \tag{A8}$$

where A_1 and A_2 depend on S, D, and T. In the limit $D \to 0$ we have from Eq. (A2),

$$A_1 = (S+1)/3S \quad (D=0) \tag{A9a}$$

and

$$A_2 = -(S+1)(2S^2+2S+1)/90S^3, \quad (D=0). \tag{A9b}$$

When $D \neq 0$, we expand A_1 and A_2 in powers of y and retain terms up to order y. In that case, A_1 and A_2 have the form

$$A_1 = [(S+1)/3S][1 + a_1 (D/kT)] \tag{A10a}$$

and

$$A_2 = -[(S+1)(2S^2+2S+1)/90S^3][1 + a_2 (D/kT)], \tag{A10b}$$

where a_1 and a_2 are numerical factors which depend on S. Thus, the analog of Eq. (A2) in the presence of anisotropy and when $\vec{H}_{eff} \| \vec{n}$ has the form

$$\bar{\mu} = \mu_0 \left[\frac{S+1}{3S} \left(1 + a_1 \frac{D}{kT} \right) x - \frac{(S+1)(2S^2+2S+1)}{90S^3} \left(1 + a_2 \frac{D}{kT} \right) x^3 \right] \equiv \mu_0 F_{\|}(x). \tag{A11}$$

Evaluation of the sums in Eq. (A7) for some special cases leads to the values

$$a_1 = \tfrac{1}{3}, \quad a_2 = 1 \quad \text{for } S = 1 \tag{A12}$$

$$a_1 = \tfrac{7}{5}, \quad a_2 = \tfrac{53}{13} \quad \text{for } S = 2 \tag{A13}$$

and

$$a_1 = \tfrac{4}{15} S^2 , \quad a_2 = \tfrac{16}{21} S^2 \quad \text{for } S = \infty . \tag{A14}$$

In the last case, while S tends to infinity, DS^2 is assumed to remain finite.

2. $\vec{H}_{eff} \perp \vec{n}$

We now show that the analog of Eq. (A2) in the presence of anisotropy and when $\vec{H}_{eff}$ is normal to $\vec{n}$ is

$$\bar{\mu} = \mu_0 \left[\frac{S+1}{3S} \left(1 + a_1^* \frac{D}{kT} \right) x - \frac{(S+1)(2S^2+2S+1)}{90S^3} \left(1 + a_2^* \frac{D}{kT} \right) x^3 \right] \equiv \mu_0 F_{\perp}(x), \tag{A15}$$

where

$$a_1^* = -\tfrac{1}{2} a_1 , \quad a_2^* = -\tfrac{1}{2} a_2 . \tag{A16}$$

To prove this result it is first useful to rewrite Eq. (A7), for $\vec{H}_{eff} \| \vec{n}$, as

$$\bar{\mu} = \frac{\mu_0}{S} \frac{\sum_m m(1 + \beta D m^2)\, e^{\beta m g \mu_B H_{eff}}}{\sum_m (1 + \beta D m^2)\, e^{\beta m g \mu_B H_{eff}}} , \tag{A17}$$

where we have retained terms up to order DS^2/kT and have let $\beta = 1/kT$. To prove Eqs. (A15) and (A16) it is only necessary to show that if $\vec{H}_{eff}$ is normal to $\vec{n}$ then, to first order in y, $\bar{\mu}$ is given by

$$\bar{\mu} = \frac{\mu_0}{S} \frac{\sum_m m(1 - \frac{1}{2}\beta D m^2)\, e^{\beta m g \mu_B H_{eff}}}{\sum_m (1 - \frac{1}{2}\beta D m^2)\, e^{\beta m g \mu_B H_{eff}}} . \tag{A18}$$

Let the x axis be normal to $\vec{n}$ and let $|p\rangle$ be the eigenstates of the operators S_x and S^2 with eigenvalues p and $S(S+1)$, respectively. In the presence of an effective field directed along the x axis the average magnetic moment per spin is given by

$$\bar{\mu} = \frac{\mu_0}{S} \frac{\sum_p \langle p | S_x e^{\beta(g\mu_B S_x H_{eff} + DS_z^2)} | p \rangle}{\sum_p \langle p | e^{\beta(g\mu_B S_x H_{eff} + DS_z^2)} | p \rangle} . \tag{A19}$$

We now use the relation[18]

$$\frac{\partial e^{-\beta\mathcal{H}}}{\partial \theta} = -\int_0^\beta e^{-(\beta-u)\mathcal{H}} \frac{\partial \mathcal{H}}{\partial \theta} e^{-u\mathcal{H}}\, du . \tag{A20}$$

Letting $\theta = D$ and expanding $e^{-\beta\mathcal{H}}$ in powers of y, we obtain to first order in y,

$$e^{\beta(g\mu_B S_x H_{eff} + DS_z^2)} = e^{\beta g \mu_B S_x H_{eff}} + D \int_0^\beta e^{(\beta-u) g \mu_B S_x H_{eff}}$$

$$\times \quad S_z^2 e^{ug\mu_B S_x H_{eff}} du . \qquad \text{(A21)}$$

Substituting Eq. (A21) into Eq. (A19), one obtains after some manipulations

$$\bar{\mu} = \frac{\mu_0}{S} \frac{\sum_p p(1+\beta D\langle p|S_z^2|p\rangle) e^{\beta p g \mu_B H_{eff}}}{\sum_p (1+\beta D\langle p|S_z^2|p\rangle) e^{\beta p g \mu_B H_{eff}}} . \qquad \text{(A22)}$$

We now use the result

$$\langle p|S_z^2|p\rangle = \tfrac{1}{2}S(S+1) - \tfrac{1}{2}p^2 , \qquad \text{(A23)}$$

and let

$$1+\beta D\left[\tfrac{1}{2}S(S+1) - \tfrac{1}{2}p^2\right]$$

$$= [1+\tfrac{1}{2}\beta DS(S+1)][1-\tfrac{1}{2}\beta D p^2] + O(y^2) . \qquad \text{(A24)}$$

Using Eqs. (A22)–(A24), one obtains to first order in y

$$\bar{\mu} = \frac{\mu_0}{S} \frac{\sum_p p[1-\tfrac{1}{2}\beta D p^2] e^{\beta p g \mu_B H_{eff}}}{\sum_p [1-\tfrac{1}{2}\beta D p^2] e^{\beta p g \mu_B H_{eff}}} . \qquad \text{(A25)}$$

Equation (A25) is identical to Eq. (A18) which we sought to prove.

B. Néel Temperature

We consider a uniaxial antiferromagnet, of the easy-axis type ($D>0$), and examine the effect of D on T_N. We assume that there are two sublattices and that the intrasublattice exchange interaction is negligible compared to the intersublattice exchange interaction.

The effective field acting on sublattice No. 1 is given by

$$\vec{H}_{eff}^{(1)} = \vec{H} - \lambda \vec{M}_2 , \qquad \text{(A26)}$$

where λ is the intersublattice exchange constant which is related to J_1 by the expression

$$\lambda = 2z_1|J_1|/Ng^2\mu_B^2 . \qquad \text{(A27)}$$

Here N is the number of spins per sublattice per cm^3.

In the absence of an external magnetic field $\vec{H}$ the sublattice magnetizations are both equal to $N\bar{\mu}$, where $\bar{\mu}$ satisfies Eq. (A7) with $H_{eff} = \lambda N\bar{\mu}$. At a temperature which is smaller than T_N by an infinitesimal amount, $\bar{\mu}$ is infinitesimally small and is given by the first term on the right of Eq. (A11). Thus,

$$\bar{\mu} = \mu_0 \left(\frac{(S+1)[1+(a_1 D/kT)] Ng\mu_B \lambda \bar{\mu}}{3kT} \right) . \qquad \text{(A28)}$$

Solving for T, one obtains for the Néel temperature

$$kT_N(D) = \tfrac{1}{3}Ng^2\mu_B^2 S(S+1)\lambda[1+a_1 D/kT_N(D)] . \qquad \text{(A29)}$$

Using Eq. (A27), one then obtains

$$kT_N(D) = \tfrac{2}{3}z_1 |J_1| S(S+1)[1+a_1 D/kT_N(D)]. \qquad \text{(A30)}$$

When $D=0$, Eq. (A30) reduces to Eq. (4). For FeF_2, $S=2$ and Eq. (A30) gives

$$T_N(D) = T_N(0)[1+7D/5kT_N(D)]. \qquad \text{(A31)}$$

The last equation agrees with the results of Ohlmann and Tinkham.[3] Using[5] $J_1 = -2.62\,^\circ K$ and $D = 9.3\,^\circ K$, one then obtains $T_N(0) = 83.8\,^\circ K$, and $T_N(D) = 95.2\,^\circ K$ (to first order in y). Computer calculations by Misetich,[8] in which higher orders of y were included, gave $T_N(D) = 95.5\,^\circ K$.

It is interesting to consider what the Néel temperature $T_N^*(D)$ would have been if the sublattice magnetizations had been forced to lie in the plane normal to $\vec{n}$. Using Eqs. (A15) and (A16), one can show that to first order in y

$$T_N^*(D) = T_N(0)[1 - a_1 D/2kT_N^*(D)] . \qquad \text{(A32)}$$

One can also show that if the boundary between the SF and P phases (in the case $\vec{H} \| \vec{n}$) is extrapolated towards the T axis, then it will intersect this axis at $T_N^*(D)$. The last statement is based on calculations to first order in y.

C. P-AF Boundary for $\vec{H} \| \vec{n}$

We assume that $\vec{H} \| \vec{n}$ and that T is just below $T_N(D)$. In the AF phase the magnetizations $\vec{M}_1$ and $\vec{M}_2$ of the two sublattices are parallel or antiparallel to $\vec{n}$ and are determined by the self-consistent solution to the pair of equations

$$\vec{n}\cdot\vec{M}_1(H,T) = Ng\mu_B S F_{||}[g\mu_B S(H - \lambda \vec{n}\cdot\vec{M}_2)/kT] \qquad \text{(A33a)}$$

and

$$\vec{n}\cdot\vec{M}_2(H,T) = Ng\mu_B S F_{||}[g\mu_B S(H - \lambda \vec{n}\cdot\vec{M}_1)/kT], \qquad \text{(A33b)}$$

where the function $F_{||}(x)$ is defined in Eq. (A11).

The P-AF transition occurs at the lowest field for which $\vec{M}_1 = \vec{M}_2$. At the transition, both $\vec{M}_1$ and $\vec{M}_2$ are parallel to $\vec{n}$. When H is lower than the transition field by an infinitesimal amount, the difference $M_1 - M_2$, calculated from Eqs. (A33), is

$$M_1 - M_2 = \frac{Ng^2\mu_B^2 S^2 \lambda (M_1 - M_2)}{kT} \frac{dF_{||}(x)}{dx} . \qquad \text{(A34)}$$

This gives

$$1 = [N\lambda g^2\mu_B^2 S(S+1)/3kT] \left((1 + a_1 D/kT) - \frac{(2S^2+2S+1)g^2\mu_B^2 (H - \lambda M_t)^2 (1 + a_2 D/kT)}{10k^2T^2} \right) , \qquad \text{(A35)}$$

where M_t is the sublattice magnetization at the transition. From Eqs. (A29) and (A35)

$$1 = \frac{T_N(D)}{T} \left(\frac{1 + a_1 D/kT}{1 + a_1 D/kT_N(D)} \right)$$

$$\times\left(1-\frac{(2S^2+2S+1)g^2\mu_B^2(H-\lambda M_t)^2(1+a_2D/kT)}{10(1+a_1D/kT)k^2T^2}\right). \tag{A36}$$

Retaining terms up to order D/kT, one obtains

$$[T_N(D)-T]\left(1+\frac{a_1D}{kT}\right)$$

$$=\frac{(2S^2+2S+1)g^2\mu_B^2(H-\lambda M_t)^2(1+a_2D/kT)T_N(D)}{10(1+a_1D/kT)k^2T^2}\,. \tag{A37}$$

At the P-AF transition, $M_1=M_2=M_t$ and M_t satisfies the relation

$$M_t=Ng\mu_BSF_{\parallel}[g\mu_BS(H-\lambda M_t)/kT]\ , \tag{A38}$$

which for T near $T_N(D)$ and for $g\mu_BSH\ll kT$ has the approximate solution

$$M_t=H/2\lambda\ . \tag{A39}$$

Substituting Eq. (A39) into Eq. (A37) and evaluating the result near $T_N(D)$ using Eq. (A30) one obtains

$$T_N(D)-T=\left(\frac{3(2S^2+2S+1)g^2\mu_B^2H^2}{80kz_1|J_1|S(S+1)}\right)\frac{1+a_2D/kT_N(D)}{[1+a_1D/kT_N(D)]^3}, \tag{A40}$$

which, to first order in D/kT_N, can also be written as

$$T_N(D)-T=\left(\frac{3(2S^2+2S+1)g^2\mu_B^2H^2}{80kz_1|J_1|S(S+1)}\right)\left(1+\frac{(a_2-3a_1)D}{kT_N(D)}\right). \tag{A41}$$

When $D=0$, either of Eqs. (A40) and (A41) leads to Eqs. (1) and (2) in the text.

Using Eqs. (A41) and (A12) one concludes that, for $S=1$, the anisotropy has no effect on the coefficient $C_{\parallel}$, to first order in D/kT. For $S=2$, Eqs. (A41) and (A13) give

$$C_{\parallel}(D)=C_{\parallel}(0)[1-8D/65kT_N(D)]\quad(S=2)\ . \tag{A42}$$

Evaluating Eq. (A42) for FeF_2 one obtains $C_{\parallel}(D)=0.99C_{\parallel}(0)$, whereas Eq. (A40) gives $C_{\parallel}(D)=0.95\,C_{\parallel}(0)$. The difference between these two values arises from the fact that in FeF_2 the factors a_1D/kT and a_2D/kT are not very small compared to unity, in which case Eq. (A42) is not equivalent to Eq. (A40). Computer calculations to all orders in D/kT show that, for FeF_2, $C_{\parallel}(D)$ does not differ from $C_{\parallel}(0)$ by more than 2%.[8]

For $S=\infty$ (classical limit), Eqs. (A41) and A14) give

$$C_{\parallel}(D)=C_{\parallel}(0)[1-4DS^2/105kT_N(D)]\quad(S=\infty). \tag{A43}$$

D. P-AF Boundary for $\vec{H}\perp\vec{n}$

The term $-DS_z^2$ in the single-ion Hamiltonian causes the free energy of the antiferromagnet to depend on the orientation of the sublattice magnetizations relative to $\vec{n}$. The dependence of this anisotropy energy on temperature was calculated in the MFA by Yosida.[17] His result for the anisotropy energy per spin $\bar{\kappa}$ is

$$\bar{\kappa}=\kappa\sin^2\theta=DS^2\left(\frac{S+1}{S}-3B_S(X)\frac{1}{2S}\coth\frac{X}{2S}\right)\sin^2\theta\,, \tag{A44}$$

where θ is the angle between the sublattice magnetization and $\vec{n}$, and X is given by

$$X=\frac{2z_1|J_1|S^2}{kT}\frac{\bar{\mu}}{\mu_0}=\frac{3}{S+1}\frac{T_N(0)}{T}\frac{\bar{\mu}}{g\mu_B}\ . \tag{A45}$$

We shall need expressions for κ at temperatures near T_N, in which case $X\ll 1$. Expanding Eq. (A44) in powers of X and retaining terms up to X^4, one obtains

$$\kappa=D(\tfrac{1}{6}X^2-\tfrac{1}{24}X^4)\quad\text{for } S=1 \tag{A46}$$

$$\kappa=D(\tfrac{21}{40}X^2-\tfrac{53}{640}X^4)\quad\text{for } S=2 \tag{A47}$$

and

$$\kappa=DS^2(\tfrac{1}{15}X^2-\tfrac{2}{315}X^4)\quad\text{for } S=\infty\ . \tag{A48}$$

Suppose a magnetic field $\vec{H}$ is applied along the x axis (normal to $\vec{n}$). In the AF phase each of the sublattice magnetizations makes an angle θ with $\vec{n}$ (or $-\vec{n}$), where[19]

$$\sin\theta=H/(2\lambda M_1+2N\kappa/M_1)\ . \tag{A49}$$

The quantity $2N\kappa/M_1$ is called the anisotropy field H_A. The P-AF transition occurs when $\vec{M}_1$ and $\vec{M}_2$ become parallel to $\vec{H}$, at which point $\theta=90°$. Hence, the condition for the transition is

$$H=2\lambda M_1[1+(N\kappa/\lambda M_1^2)]\ . \tag{A50}$$

To obtain an equation for the P-AF boundary we shall consider the equation for $\bar{\mu}$ in the P phase and then we shall impose condition (A50).

We specialize to the case $S=2$. From Eqs. (A4), (A13), (A15), and (A16) the equation for $\bar{\mu}$ in the P phase is

$$\bar{\mu}=\mu_0\left[\left(\frac{\mu_0H_{\rm eff}}{2kT}\right)\left(1-\frac{7D}{10kT}\right)-\frac{13}{240}\left(\frac{\mu_0H_{\rm eff}}{kT}\right)^3\left(1-\frac{53D}{26kT}\right)\right]\ , \tag{A51}$$

where

$$H_{\rm eff}=H-N\lambda\bar{\mu}\ . \tag{A52}$$

From Eqs. (A50) and (A52),

$$H_{\rm eff}=N\lambda\bar{\mu}+(2\kappa/\bar{\mu}). \tag{A53}$$

For $S=2$, Eq. (A45) gives

$$X=[T_N(0)/T](\bar{\mu}/g\mu_B)\ . \tag{A54}$$

From Eqs. (A47), (A53), and (A54) one obtains

$$H_{eff} = N\lambda\bar{\mu}\left\{1 + \frac{D}{kT}\left[\frac{21T_N(0)}{10T} - \frac{53}{160}\left(\frac{T_N(0)}{T}\right)^3 \frac{\bar{\mu}^2}{g^2\mu_B^2}\right]\right\}. \quad \text{(A55)}$$

In deriving Eq. (A51) we retained terms up to order $x^3 = (\mu_0 H_{eff}/kT)^3$ which, when $x \ll 1$, is of order $(\bar{\mu}/\mu_0)^3$. If we factor out $\mu_0 H_{eff}/kT$ in Eq. (51) and use Eq. (A55) we obtain

$$\bar{\mu} = \frac{2N\lambda g^2\mu_B^2\bar{\mu}}{kT}\left[1 + \frac{D}{kT}\left(\frac{21T_N(0)}{10T} - \frac{7}{10}\right) - \frac{53}{160}\left(\frac{T_N(0)}{T}\right)^3 \frac{\bar{\mu}^2}{g^2\mu_B^2}\frac{D}{kT} - \frac{13}{120}\left(\frac{\mu_0 H_{eff}}{kT}\right)^2 \times \left(1 - \frac{53D}{26kT} + \frac{21DT_N(0)}{10kT^2}\right)\right], \quad \text{(A56)}$$

where we have neglected terms involving $(D/kT)^2$ and a term of order $(\bar{\mu}/\mu_0)^5$. The Néel temperature is obtained from Eq. (A56) by letting $\bar{\mu}$ be infinitesimally small, which gives

$$kT_N(D) = 2N\lambda g^2\mu_B^2\left[1 + \frac{D}{kT_N(D)}\left(\frac{21T_N(0)}{10T_N(D)} - \frac{7}{10}\right)\right]. \quad \text{(A57)}$$

To first order in D/kT_N, Eq. (A57) can be written as

$$kT_N(D) = 2N\lambda g^2\mu_B^2\left[1 + 7D/5kT_N(D)\right]. \quad \text{(A58)}$$

The last equation agrees with Eq. (A31).

Equation (A56) can be written as

$$T_N(0)\left[1 + \frac{D}{kT}\left(\frac{21T_N(0)}{10T} - \frac{7}{10}\right)\right] - T = \frac{13T_N(0)}{120}\left(\frac{\mu_0 H_{eff}}{kT}\right)^2\left(1 - \frac{53D}{26kT} + \frac{21DT_N(0)}{10kT^2} + \frac{159}{52}\frac{DT_N(0)}{kT^2}\right), \quad \text{(A59)}$$

where terms of order $(D/kT)^2$ were neglected. From Eq. (A57) it follows that the left side of (A59) vanishes at $T_N(D)$. Expanding this left side about $T_N(D)$, we obtain to first order in $T_N(D) - T$,

$$[T_N(D) - T]\left[1 + \frac{D}{kT_N(D)}\left(\frac{21T_N^2(0)}{5T_N^2(D)} - \frac{7T_N(0)}{10T_N(D)}\right)\right]. \quad \text{(A60)}$$

In evaluating the right-hand side of Eq. (A59), we use the relation

$$H_{eff} = \tfrac{1}{2}[H + (2\kappa/\bar{\mu})], \quad \text{(A61)}$$

which is obtained from Eqs. (A52) and (A53). Then, to first order in D/kT,

$$H_{eff} = \frac{H}{2}\left(1 + \frac{\kappa}{N\lambda\bar{\mu}^2}\right) = \frac{H}{2}\left(1 + \frac{21}{20}\frac{D}{kT}\frac{T_N(0)}{T}\right), \quad \text{(A62)}$$

where we used Eqs. (A47) and (A54) and have neglected a term of order $H_{eff}(D/kT)(\bar{\mu}/\mu_0)^2$. From Eqs. (A58)–(A60) and (A62), one obtains, to first order in D/kT and for T near $T_N(D)$,

$$T_N(D) - T = \frac{13g^2\mu_B^2H^2}{120k^2T_N(0)}\left(1 - \frac{281}{260}\frac{D}{kT_N(D)}\right). \quad \text{(A63)}$$

The second term in the parenthesis of Eq. (A63) gives the effect of the anisotropy on the coefficient $C_{\parallel}$. For FeF_2, using the value $D = 6.5\ cm^{-1}$ and the calculated value $T_N(D) = 95\ ^\circ K$, one obtains from Eq. (A63), $C_{\parallel}(D) \cong 0.89C_{\parallel}(0)$.

In the case $S = \infty$, a calculation similar to the one above gives

$$T_N(D) - T = \frac{\mu_0^2H^2}{60k^2T_N(0)}\left(1 - \frac{22}{105}\frac{DS^2}{kT_N(D)}\right). \quad \text{(A64)}$$

---

*Supported by the U. S. Air Force Office of Scientific Research.

[1]Y. Shapira and S. Foner, Phys. Rev. B 1, 3083 (1970).

[2]Y. Shapira, Phys. Letters 30A, 388 (1969).

[3]R. C. Ohlmann and M. Tinkham, Phys. Rev. 123, 425 (1961).

[4]M. E. Lines, Phys. Rev. 156, 534 (1967); 156, 543 (1967).

[5]H. J. Guggenheim, M. T. Hutchings, and D. B. Rainford, J. Appl. Phys. 39, 1120 (1968).

[6]E. Catalano and J. W. Stout, J. Chem. Phys. 23, 1803 (1955); 23, 2013 (1955).

[7]F. Keffer, Phys. Rev. 87, 608 (1952).

[8]A. Misetich (private communication).

[9]J. Skalyo, Jr., A. F. Cohen, S. A. Friedberg, and R. B. Griffiths, Phys. Rev. 164, 705 (1967).

[10]M. E. Fisher, Phil. Mag. 7, 1731 (1962).

[11]Y. Shapira and J. Zak, Phys. Rev. 170, 503 (1968).

[12]B. Lüthi and R. J. Pollina, Phys. Rev. 167, 488 (1968).

[13]M. Barmatz and I. Rudnick, Phys. Rev. 170, 224 (1968).

[14]J. W. Stout and M. Yuzuri (private communication).

[15]S. Foner, in *Proceedings of the International Conference on Magnetism, Nottingham*, 1964 (The Institute of Physics and the Physical Society, London, 1964), p. 438.

[16]T. Tanaka, L. Libelo, and R. Kligman, Phys. Rev. 171, 531 (1968).

[17]K. Yosida, Progr. Theoret. Phys. (Kyoto) 6, 691 (1951).

[18]R. M. Wilcox, J. Math. Phys. 8, 962 (1967).

[19]T. Nagamiya, K. Yosida, and R. Kubo, Advan. Phys. 4, 1 (1955).